

A Joint DLR-ONERA Contribution to CFD-based Investigations of Unconventional Empennages for Future Civil Transport Aircraft

Gérald CARRIER¹ and Lutz GEBHARDT²

¹ ONERA, Applied Aerodynamics Department
BP72, 92322 Châtillon Cedex, France, e-mail: gerald.carrier@onera.fr

² DLR, Institute of Aerodynamics and Flow Technology
D-38108 Braunschweig, Germany, e-mail: lutz.gebhardt@dlr.de

Summary

The introduction of innovative empennage configurations on transonic transport aircraft may potentially improve their aerodynamic performance due to a reduction of the wetted surface and a corresponding decrease in drag. This paper describes the CFD analysis performed at DLR and ONERA in the context of the European research project NEFA to investigate some key aerodynamics features related to alternative tail configurations. Emphasis is placed on the aerodynamic performance at cruise flight conditions of three tail variants of an otherwise identical aircraft: a conventional tail, a U-tail and a V-tail empennage. The results obtained confirm the potential aerodynamic benefits of the V-tail configuration and show that the U-tail has about the same performance as the conventional tail.

1 Introduction

To satisfy stability, controllability and handling qualities requirements, conventional aircraft designs include empennage-mounted tail surfaces. With current transport aircraft types, these tail surfaces consist of a combination of a vertical and a horizontal tail plane (VTP and HTP). This conventional tail configuration has the advantage of decoupling, to a large extent, the longitudinal and lateral effects of control surface deflections. However this layout is also responsible for a considerable part of the wetted area of the aircraft (and consequently friction drag), in addition to the interference drag resulting from the intersections of the three tail surfaces with the fuselage. Alternative tail configurations may potentially improve the aerodynamic performance of an aircraft while still maintaining an equivalent tail authority. In the case of the V-tail, the potential aerodynamic benefits are the result of a reduction in wetted surface area and in interference drag (only two instead of three tail surfaces have to be mounted on the fuselage). The drag reduction potential of the U-tail is not likely to be very high as a large reduction in wetted area does not seem possible. On the other hand, interference drag may be lower due to the reduced number of intersections with the fuselage. As the U-tail offers benefits from a noise shielding

perspective for aft mounted engines, it may be a worthwhile alternative to a conventional tail if it does not incur a noticeable drag penalty in comparison.

The objective of this paper is to analyse the potential benefits that can be offered by V- and U-tail configurations in terms of aerodynamic performance at cruise flight conditions compared to a conventional tail concept. After introducing the European research project NEFA as part of which the work presented has been carried out, the aircraft used for these investigations is briefly described. Then lift and drag characteristics are compared and evaluated, followed by a section with special emphasis on the analysis of the V-tail with regard to trim drag development and aerodynamic performance in comparison to the reference tail.

2 The European Research Project NEFA

The ongoing European research project “New Empennage For Aircraft” (NEFA) has been set up to study the overall impact of new empennage concepts on the performance and handling qualities of a transport aircraft. In this project, V- and U-tail layouts are investigated that may provide performance and other improvements over conventional tails used today and thereby contribute to achieving the goals defined in the European Vision 2020 (reduction of CO₂ by 50%, NO_x by 80% etc.). Because alternative tail concepts will have a wide-ranging impact on many aspects of the aircraft, the multi-disciplinary trade-off between aerodynamics, structural weight changes, and handling qualities issues are investigated in the NEFA project.

The aerodynamics work package of NEFA (WP2) is intended to provide accurate evaluations of the tail configuration effect on the aerodynamic performance and on the handling qualities of the aircraft, and to give insight into the flow phenomena occurring with these unconventional tail designs using both CFD and experimental investigations. Within this work-package, ONERA and DLR are applying their expertise in aerodynamics and CFD to support the evaluation of the impact of new empennage types on the aircraft aerodynamics, together with partners from several European countries: Airbus in France, Spain and Germany, Helsinki University of Technology (HUT) in Finland, Instituto Nacional de Tecnica Aeroespacial (INTA) in Spain and the Technical University of Braunschweig (TUBS) in Germany.

3 Aircraft Configuration, Tail Design and Flight Conditions

Starting from a conventional short-to-medium range transonic transport aircraft design representative of the 100-seat class with a cruise Mach number of $M=0.77$ and equipped with a conventional horizontal and vertical tail (the reference tail), two alternative tail variants, respectively a V-tail and a U-tail were defined in the first work package of the project. These tail configurations are the result of a multidisciplinary preliminary design optimization performed by the Future Projects Offices of Airbus in France and Germany with the constraint of yielding

equivalent, certifiable handling qualities and taking into account several important design aspects like weight, handling qualities, aerodynamics, engine characteristics, mission profile, etc... . This was followed by a refinement loop through detailed aerodynamic design work done at Airbus Germany in Bremen. The final V-tail design is a trimmable V-tail in combination with a modified empennage in the tail-to-fuselage junction area to account for the acute angle between tail and fuselage and the higher absolute thickness of the V-tail at the intersection with the fuselage. A graphical comparison of these configurations is depicted in Figure 1. All results presented in this paper correspond to cruise flight conditions as realized during the high speed wind tunnel tests performed as part of NEFA ($Re=2.7 \times 10^6$).

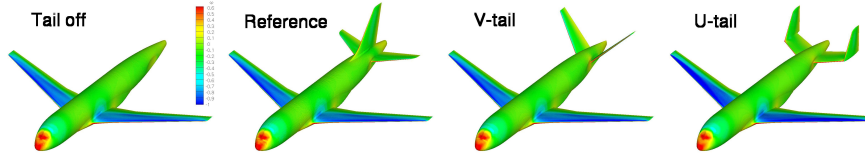


Figure 1: View of the 4 different tail configurations investigated. Pressure distributions from RANS calculations at $M=0.77$, $C_L=0.4$, $Re=2.7 \times 10^6$.

4 Methods

All aerodynamic investigations presented were carried out with the DLR TAU code [1], a solver for the Reynolds-averaged Navier-Stokes equations for hybrid meshes, using the Spalart-Allmaras turbulence model with Edwards modification. The ONERA FFD70 drag post-processor, based on far-field analysis [2, 3] has been applied to post-process some of the solutions calculated with the TAU code.

5 Comparison of Reference-, U-, and V-tail Characteristics

The calculation of tail polars and efficiencies requires a rather large number of computations at different combinations of tail incidence settings and aircraft angle of attack. Therefore it was necessary to create hybrid meshes for the NS-solver TAU with a reasonable number of grid points, for which the commercial mesh generation package CENTAUR was used [4]. Using identical mesh generation parameters in order to keep the solutions comparable, grid sizes between 1.6 million nodes for the tail-off configuration and 2.3 millions for the U-tail configuration were achieved.

For symmetric onset flow conditions ($\beta=0^\circ$), calculations at different aircraft angle of attack α were performed for the tail-off configuration and in combination with three tail incidence settings i_H . The surface pressure distribution calculated by TAU was integrated to obtain forces and moments using the DLR tool Aeroforce [5]. Because this tool allows an easy definition of split planes, data analysis could be done in a similar way to the Live Rear End (LRE) technique used in the wind tunnel investigations. A split plane is defined perpendicular to the fuselage axis

between wing and tail, and the forces and moments of all parts behind the split plane are summed up. By subtracting the results from the calculations with and without tail, values for the isolated tail are obtained while taking installation effects and the downstream effect of wing and fuselage into account.

5.1 Determination of Downwash and Efficiency

In order to determine the tail plane efficiencies $\delta C_{LH}/\delta \alpha_H$, the mean downwash angle ϵ at the location of the tail must be computed first. ϵ can then be used to calculate α_H from α and i_H :

$$\alpha_H = \alpha - \epsilon + i_H \quad (1)$$

This procedure assumes that lift, drag, moment and downwash change in a linear manner with α which means that the aircraft angles of attack α used and tail incidence settings i_H must be sufficiently small in order stay in the linear regime. Other phenomena which lead to non-linear behaviour like the occurrence of shocks and/or separation must also be avoided. The distribution of C_{LH} vs. α resulting from Eq. (1) is plotted in Figure 2.

	$\delta C_{LH}/\delta \alpha_H$	ϵ_0	$\delta \epsilon/\delta \alpha$	$S_{HTP}/S_{ref} * \delta C_{LH}/\delta \alpha_H * (1 - \delta \epsilon/\delta \alpha)$
Ref. Tail	4.39	0.61	0.42	0.71
U-Tail	4.08	1.75	0.38	0.70
V-Tail	2.77	0.45	0.33	0.65

Table 1: Comparison of lift curve slope, downwash and efficiency

The lift curve slope is usually taken as a measure for a tail's efficiency. In this regard, Figure 2 indicates that the reference tail has the highest efficiency, closely followed by the U-tail. This may be attributed partly to the lower aspect ratio of the U-tail HTP which is not completely offset by the two VTP's which act as winglets, i.e. increase the effective aspect ratio of the U-tail HTP. When referencing the lift curve slope to aircraft (not HTP) reference values, the two tails are almost identical in performance due to the smaller downwash coefficient of the U-tail in comparison to the reference tail (see Table 1). The V-tail efficiency on the other hand is noticeably lower, mainly due to the fact that the actual tail surface area is used as reference area for all configurations while only part of this area acts in vertical direction due to the high dihedral angle of the V-tail (43.1°) in comparison to the other tail shapes (6°). Like in the case of the U-tail, this reduced efficiency is partly offset by a lower downwash gradient, which can be attributed to the fact that a large part of the V-tail has a greater vertical distance from the wing wake location in the tail area.

5.2 Lift and Drag Characteristics

The dataset collected for the computation of the tail efficiencies can also be used to determine the tail drag polar. With C_{LH} already available, C_{DH} is calculated also

using the LRE method. A set of computations at different α but identical i_H results in one “branch” of the drag polar. If several branches for different i_H are plotted in one diagram, one observes that the branches do not join each other. This is due to different effective α_H for different i_H as a change in i_H also results in a change of the HTP position in the wing wake, which in turn results in a different downwash value at the tail. Therefore C_{LH} and C_{DH} must be corrected for ε as follows:

$$C_{LH,\alpha_H} = C_{LH,\alpha} \cdot \cos \varepsilon + C_{DH,\alpha} \cdot \sin \varepsilon \quad (2)$$

$$C_{DH,\alpha_H} = C_{DH,\alpha} \cdot \cos \varepsilon - C_{LH,\alpha} \cdot \sin \varepsilon$$

Using values of ε determined from two successive calculation points, the branches for the different tail incidence settings join each other reasonably well (Figure 3).

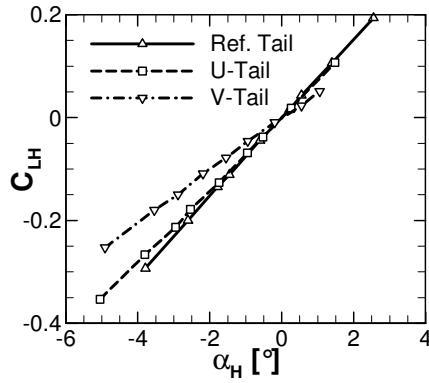


Figure 2: Comparison of the lift curve slope of the three tail configurations

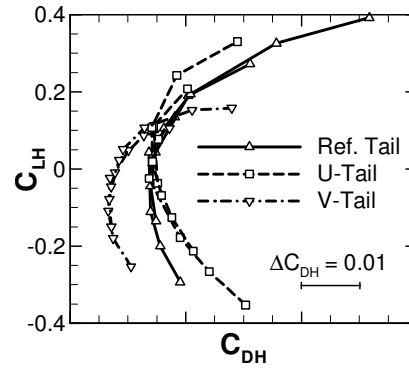


Figure 3: Tail drag polars for reference tail, U-tail and V-tail

Analysing the drag polars, some interesting conclusions can be drawn. First, reference tail and U-tail have similar minimum drag values, while C_{LH} for minimum drag is shifted to more positive C_{LH} values. Also, C_{DH} rises faster with increasing negative C_{LH} -value for the U-tail which is not as desirable as the behaviour of the reference tail. As the design effort put into the U-tail configuration was lower than for the reference or V-tail configuration, it seems likely that there is still some potential in the U-tail which could be used to adjust the shape of its drag polar. Even in the current state, the U-tail does not exhibit any negative characteristics from an aerodynamic point of view which would preclude its use on an actual aircraft configuration which might be beneficial for example for noise shielding purposes in combination with aft mounted engines[6].

The drag polar of the V-tail highlights its aerodynamic advantages in comparison to the two other tail shapes. It has a considerably lower minimum drag value at slightly negative C_{LH} values and very low drag variation between $C_{LH}=0$ and $C_{LH}=-0.2$. Drag rises faster for positive C_{LH} in relation to the reference tail, but up to about $C_{LH}=+0.1$ the drag of the V-tail is nevertheless lower.

6 Trim Drag Analysis of the V-tail Configuration

To be able to trim the aircraft for different location of the centre of gravity (C.G.), the tail is used as a trimming surface which produces a lift and therefore a corresponding lift-induced drag contribution. For a conventional tail, the lift-induced drag due to trim is produced by the horizontal tail plane (HTP). With a relatively low dihedral angle, a conventional HTP behaves similarly to a conventional planar lifting surface (placed in the downwash of the main wing) and therefore its behaviour is sufficiently well known and modelled today. In the case of a V-tail design with a dihedral angle close to 45° , the development of the drag due to trim is expected to be more complex.

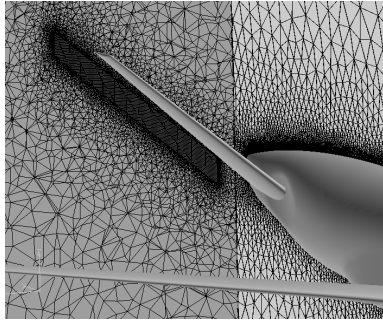


Figure 4: View of some mesh refinements included in the hybrid meshes to properly capture the tail wake.

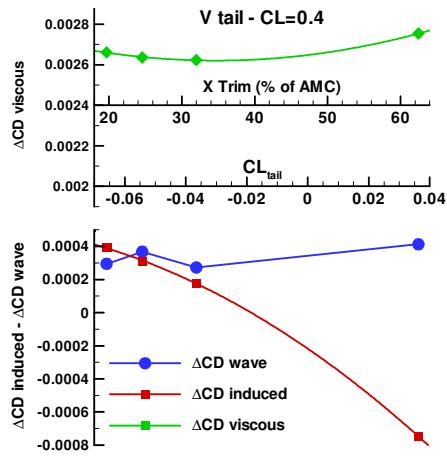


Figure 5: Evolution of the different V-tail drag components with the tail lift.

To investigate the development of the trim drag in the case of the V-tail configuration, RANS calculations have been carried out and analysed with the ONERA far-field drag extraction tool for different tail settings ranging from $i_H=0^\circ$ to $i_H=-2.8^\circ$. All calculations have been performed at the same lift condition of $C_L=0.4$, representative of a cruise condition at fixed aircraft weight. Each calculation therefore yields a different trim condition, i.e. a different location of the C.G. of the aircraft. Special effort has been made to generate hybrid CFD meshes of good quality in the region of the tail wake as illustrated in

Figure 4. The V-tail meshes consist of about 5.7 millions cells each and include a block of hexahedral cells downstream of the tail. In order to derive the trim drag due to tail lift, a calculation has also been made for the tail-off aircraft configuration for the same lift condition of $C_L=0.4$.

The application of the far-field drag extraction technique provides a breakdown of the total drag into its viscous (friction plus viscous pressure drag), wave and lift-induced components for each configuration. “Tail drag” and its different components are then defined with respect to the tail-off configuration as follows:

$$\Delta CD_X = CD_X^{Vtail} - CD_X^{Tail-off}, \quad (3)$$

with “X” representing any of the total/viscous/wave/induced drag components. The evolution of the different “tail drag” components with the location of the aircraft CG is plotted in Figure 5. Compared to the tail-off configuration, the main source of drag increase is of course the viscous drag component, explained by an 11% increase in wetted surface area. The variation of this viscous components is however limited to a specific trim condition. The lift-induced drag component exhibits the largest variations, with a 4% forward displacement of the C.G. resulting in a 1 drag count increase. It should be noted that for positive tail lift conditions (high tail setting angle), the V-tail aircraft has a lower lift-induced drag (negative value of $\Delta CD_{induced}$).

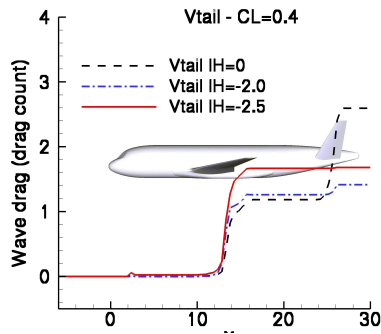


Figure 6: Streamwise wave drag development (accumulated) for the V-tail configuration at $C_L=0.4$ and 3 tail settings

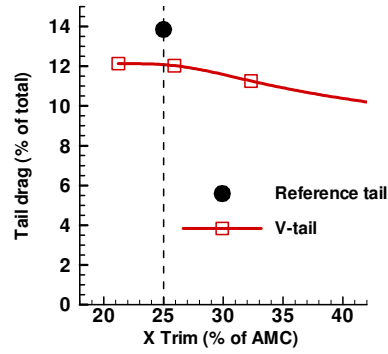


Figure 7 : Comparison of reference and V-tail drag at $C_L=0.4$ for a CG placed at 25% of the Mean Aerodynamic Chord.

Finally, the wave drag term contributes only very little to the total “tail drag” (Figure 5) and shows very small variations with a change in trim condition (about 1 drag count). The localisation of the flow regions contributing to the wave drag is also possible by means of the far-field analysis. The streamwise wave drag distribution for the V-tail aircraft at $C_L=0.4$ and at three tail settings is given in Figure 6. This shows that for the highest investigated tail setting ($i_H=0^\circ$), for which the tail has a positive lift contribution, the tail itself contributes to the total wave drag at the same level as the wing. In contrast, the tail does not noticeably contribute to the total wave drag by itself for the more negative tail settings, although it affects the wave drag produced on the wing, which can be explained by a higher wing lift required to compensate the higher negative tail lift.

7 Cruise Drag Comparison

Using the far-field drag analysis technique, accurate evaluations of the total drag for the V-tail and the reference tail configuration have been performed. The results obtained are given in Figure 7 which provides a comparison of the “tail drag” for

the V-tail and the reference tail design at $C_L=0.4$. For the trim condition with the C.G. located at 25% MAC, the V-tail design offers a 15% reduction in tail drag.

8 Conclusion

The cooperative ONERA-DLR research effort conducted within the NEFA project as presented in this paper provides insight into the aerodynamics of alternative tail types, a subject for which little recent data is available. The results of the CFD investigations at cruise conditions and wind tunnel Reynolds number clearly prove the drag reduction potential of the V-tail, which more than offsets its lower efficiency. As installation and control surface redundancy issues could be resolved through the work of other partners within NEFA, and weight estimation with high-fidelity tools does not show a weight penalty for the V-tail, this tail type seems to be the premier choice for the tail configuration of a highly efficient, low drag and consequently low-fuel consumption and low-emission aircraft. Furthermore, it was shown that the U-tail has performance characteristics similar to a conventional tail. It may therefore be used if more emphasis is put on other aircraft design aspects like shielding the noise of aft fuselage-mounted engines. The results presented will help to evaluate the potential contribution of novel empennage types to achieve the goals set forth in the European Vision 2020 for future civil transport aircraft with regard to reduced environmental impact of air traffic.

Acknowledgements

The work was performed under the European Research Contract No. G4RD-CT-2002-00864 as part of the 5th framework programme “Competitive and Sustainable Growth”. The authors would like to thank the European Commission for supporting this pre-competitive research work.

References

- [1] T. Gerhold: “Overview of the Hybrid RANS Code TAU”, *Notes on Numerical Fluid Mechanics*, edited by N. Kroll and J. Fassbender, Vol. 89, Springer 2005, pp. 81-92
- [2] D. Destarac: “Far-Field/Near-Field Drag Balance and Application of Drag Extraction in CFD”, VKI Lecture Series 2003, CFD-based Aircraft Drag Prediction and Reduction, National Institute of Aerospace, Hampton (VA), November 3-7, 2003.
- [3] J. Van Der Vooren and D. Destarac: “Drag-Thrust analysis of Jet-propelled Transonic Transport Aircraft; Definition of Physical Drag Components”, *Aerospace Science & Technology*, Vol. 8 (2004), pp. 545-556.
- [4] CentaurSoft, URL: <http://www.centaursoft.com/> [cited May 2005]
- [5] J. Wild: “AeroForce – Thrust/Drag Bookkeeping and Aerodynamic Force Breakdown over Components”. IB 129-99/9, DLR, Braunschweig, June 1999
- [6] Brodersen, O., et. al.: “Aerodynamics Investigations in the European Project ROSAS (Research on Silent Aircraft Concepts)”, AIAA Paper 2005-4891, accepted for the 23rd AIAA Applied Aerodynamics Conference, 6-9 June 2005, Toronto, Canada